

1 **Size and composition of the MORB+OIB mantle reservoir**
2

3 **A.W. Hofmann^{1,2}, C. Class² and S.L. Goldstein^{2,3}**

4 ¹Max Planck Institute for Chemistry, Hahn-Meitnerweg 1, 55128 Mainz, Germany.

5 ²Lamont-Doherty Earth Observatory of Columbia University, Palisades, New York 10964.

6 ³Department of Earth and Environmental Sciences, Columbia University, Palisades, New York
7 10964, USA.

8
9 Corresponding author: Albrecht Hofmann (Albrecht.hofmann@mpic.de)
10

11 **Key Points:**

- 12 • A new assessment of the depleted mantle mass (> 65%) based on (Nb,Ta)/U conflicts
13 with conventional estimates using Nd isotopes (<50%)
14 • This invalidates the classic 3-reservoir silicate Earth (continental crust, depleted mantle,
15 and primitive mantle).
16 • The observable, present-day mantle was permanently depleted by segregation or loss of
17 an early-enriched reservoir.
18

19 **Abstract**

20 Most efforts to characterize the size and composition of the mantle that complements the continental crust have
21 assumed that the mid-ocean ridge basalt (MORB) source is the incompatible-element depleted residue of continental
22 crust extraction. The use of Nd isotopes to model this process led to the conclusion that the “depleted MORB
23 reservoir” is confined to the upper ~30% of the mantle, leaving the lower mantle in a more “primitive” state. Here
24 we use Nb/U and Ta/U to evaluate mass and composition of the mantle reservoir residual to continent extraction and
25 find that it exceeds 67% of the total mantle. Thus the (Nb,Ta)/U-based mass balance conflicts with the $\epsilon(\text{Nd})$ -based
26 mass balance, ~~and~~ this invalidates the classical 3-reservoir silicate Earth model (continental crust, depleted mantle,
27 primitive mantle). Including the combined MORB + ocean island basalt (OIB) sources in the $\epsilon(\text{Nd})$ -based mass
28 balance does not reconcile the conflict as it would require their average $\epsilon(\text{Nd})$ to be ≤ 3.0 , much lower than observed
29 MORB+OIB $\epsilon(\text{Nd})$ averages. We resolve this conflict by invoking an additional, “early-enriched reservoir” (EER),
30 formed prior to extraction of significant continental crust, but now hidden or lost. This EER differs from EERs
31 previously invoked by having no Nb-Ta anomaly. We suggest that it originated as an early mafic crust, which had
32 unfractionated (Nb,Ta)/U but fractionated Sm/Nd ratios. The corresponding “early-depleted” reservoir (EDR)
33 generated the present-day continental crust and the “residual mantle” MORB-OIB reservoir, which occupies at least
34 70% of the present-day mantle and is only moderately depleted in incompatible trace elements.

35

36 **Plain Language Summary**

37 The Earth’s continental crust makes up only about half a percent of Earth’s mass, but it contains a large portion of
38 its total budget of uranium and thorium, which produce much of Earth’s interior heat. In making the crust, these
39 elements have been extracted via melts and volcanism from Earth’s mantle. But what portion of the mantle was
40 involved in making the continents? Previously, geochemists concluded that only its uppermost 30% was involved,
41 leaving the lower two-thirds of the mantle essentially untouched. The measure used for this estimate has been the
42 difference in the isotope ratios of neodymium, $^{143}\text{Nd}/^{144}\text{Nd}$, between crust and mantle. However, when we use an
43 alternative measure for the same calculation, namely the ratio of niobium to uranium, Nb/U, we find the depleted
44 mantle fraction to be greater than 60%. We therefore need an Earth model that involves an additional “reservoir”
45 with crust-like Nd isotopes but mantle-like Nb/U. We model this as an early Earth ocean crust, which may have
46 been lost to space, or may now be hidden at the base of the mantle. A buried ancient ocean crust might well explain
47 the large density/temperature anomalies recently discovered at the base of the mantle by seismologists.

48 **1 Introduction**

49 The upper portion of Earth’s mantle is extensively sampled by mid-ocean ridge basalts (MORBs), and its
50 composition has been estimated using isotope-based modeling and partial melting theory. Most efforts to
51 characterize the size and composition have assumed that the MORB source is the incompatible-trace-element
52 depleted residue of continental crust extraction. The use of Nd isotopes to make this estimate consistently led to the
53 conclusion that the “depleted MORB reservoir” is approximately ~30% of the mantle, which is the approximate size
54 of the upper mantle above the 670 km seismic discontinuity (e.g. Jacobsen and Wasserburg, 1979; O’Nions et al.

55 1979; DePaolo, 1980; Allègre et al., 1980; Davies, 1981). This further led to the classical three-layer (continents,
56 upper mantle, lower mantle) Earth model, whereby the upper mantle is the MORB source and the lower mantle is
57 left in a more or less “primitive” or “primordial” (i.e. undifferentiated) state. This model was supported by many
58 observations, three important ones are that the lower mantle is sampled by ocean island basalts (OIBs) and oceanic
59 plateaus, at least some of which are generated by deep-mantle plumes (e.g. French and Romanowicz, 2015); early
60 Nd isotope studies of OIB showed values between MORB and chondrites (DePaolo and Wasserburg, 1976; O’Nions
61 et al., 1977); and some of these OIBs contained high $^3\text{He}/^4\text{He}$ ratios compared to MORB, confirming their
62 primordial heritage (e.g. Farley et al., 1992).

63 While these early Nd isotope studies suggested that OIBs were derived from primitive lower mantle, no
64 OIB source has been shown to be truly primitive, and some authors concluded that the less depleted, but non-
65 primitive Nd-Sr isotopic signatures of OIBs are caused by mixing of primitive material from the lower mantle with
66 depleted material from the upper mantle during plume ascent (e.g. Wasserburg and DePaolo, 1979). The
67 combination of deep subduction and rising mantle plumes provide mechanisms for mixing upper and lower mantle,
68 but the differences between the Nd, Hf, and Sr isotopic compositions of OIBs and MORBs indicate that some
69 stratification is preserved in spite of such convective mixing. These isotopic compositions show that MORB sources
70 have been generally more depleted in incompatible trace elements over geological time than OIB sources. Much of
71 this mixing was thought to occur when a rising plume entrains the overlying mantle material (e.g. Hart et al., 1992;
72 Hauri et al. 1994; Farley et al., 1992), but Farnetani and Richards (1995) examined the entrainment process required
73 for such mixing; they found that the entrained material does not significantly contribute to the melts formed by a
74 plume that rises from the deep mantle.

75 A consequence of the classical three-reservoir (continents, MORB-mantle, primitive mantle) concept for
76 the Earth is that the currently most widely used models for the composition of the depleted MORB-source upper
77 mantle (Salters and Stracke, 2004; Workman and Hart, 2005), though different in some important details, both rely
78 on the basic assumption that the Sm/Nd ratio of this depleted mantle can be derived from its Nd isotopic
79 composition via simple crustal extraction models. In both cases, this crustal extraction is modeled in terms of crustal
80 growth through unidirectional, mantle-to-crust extraction of crustal elements through time. But any simple
81 relationship between parent-daughter ratio and radiogenic enrichment of the daughter element is lost if the actual
82 crustal history was not one of simple unidirectional growth but involved substantial recycling of crust back into the
83 mantle. Moreover, it was shown by Hofmann et al. (1986) and by Campbell (2002) that the continental crust is not
84 the only chemical complement of the depleted mantle, but that stored oceanic crust also contributes a significant
85 portion to the fractionation of Sm/Nd. These considerations cast doubts on the validity of the estimates of the
86 depleted-mantle composition based on mass balance between the continents and the MORB-mantle, and they call
87 for a re-examination of Earth’s continent-mantle mass balance. A major point of the present contribution will be to
88 show that the above approach has led to a serious underestimate of the mass of the mantle that is residual to
89 continental extraction, and a corresponding overestimate of its degree of depletion. We employ a simple mass
90 balance approach, using alternatively $\epsilon(\text{Nd})$ and $(\text{Nb,Ta})/\text{U}$ in a three reservoir silicate Earth (continental crust, a
91 depleted reservoir that may take into account OIB- as well as MORB-mantle, primitive mantle) to show that the

92 results from the $\epsilon(\text{Nd})$ based mass balance and from the $(\text{Nb,Ta})/\text{U}$ based mass balance cannot be reconciled, unless
 93 the Earth is either non-chondritic or contains an additional, hidden, enriched reservoir.

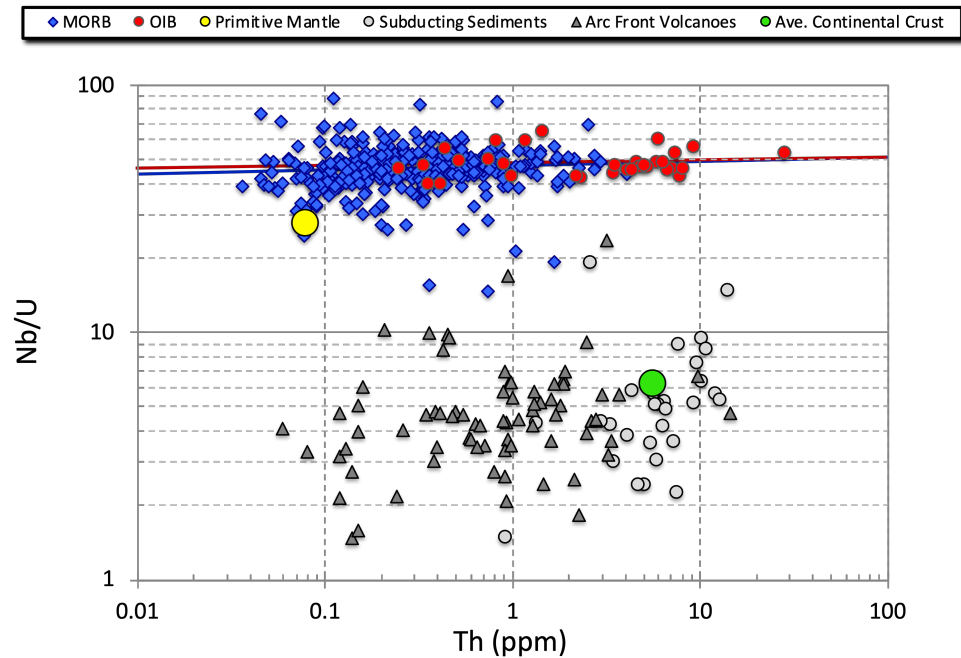
94 The idea of an additional, permanently hidden silicate reservoir, presumably located at the base of the
 95 mantle, was introduced by Tolstikhin and Hofmann (2005) on the basis of xenon isotopes, and by Boyet and Carlson
 96 (2005) on the basis of their discovery of the non-chondritic terrestrial ratio of $^{142}\text{Nd}/^{144}\text{Nd}$, reflecting the decay of the
 97 extinct nuclide ^{146}Sm . Super-chondritic $^{142}\text{Nd}/^{144}\text{Nd}$ ratios observed in both crustal and mantle rocks implied that the
 98 “accessible silicate Earth” has a superchondritic Sm/Nd ratio, which would be balanced by a subchondritic Sm/Nd
 99 located in an inaccessible Early Enriched Reservoir (EER) (Boyet and Carlson, 2005, 2006; Carlson and Boyet,
 100 2008). More recent research has shown that the ^{142}Nd -isotopic compositions of chondrites are variable and do not
 101 necessarily require a non-chondritic terrestrial Sm/Nd ratio (e.g. Burkhardt et al., 2016). We will nevertheless adopt
 102 Boyet and Carlson’s nomenclature of an Early Enriched Reservoir (EER), leaving behind an Early Depleted
 103 Reservoir (EDR), because it can reconcile our two independent mass balances for the crust-mantle system. We note,
 104 however, that our method for estimating the compositions of these reservoirs is quite different from that employed
 105 by Boyet and Carlson (2005); (see also Supporting Information).

106 Using the mass balance approach originally set out by Davies (1981), we will demonstrate that the
 107 traditional three-reservoir silicate Earth (continental crust, depleted mantle, primitive mantle) yields irreconcilable
 108 results for the mass balances employing $(\text{Nb,Ta})/\text{U}$ and $\epsilon(\text{Nd})$, respectively. We then show that simple
 109 differentiation of the depleted mantle into an even-more-depleted MORB source and a less depleted OIB source
 110 does not resolve the discrepancy. Finally, we propose a 4-reservoir model including a hidden, early-enriched
 111 reservoir somewhat similar, but not identical, to the EER proposed by Boyet and Carlson (2005, 2006) and Carlson
 112 and Boyet (2008), or the reservoir lost by accretional erosion postulated by O’Neill and Palme (2008) and Jackson
 113 and Jellinek (2013). The complementary early-depleted reservoir (EDR) will be subsequently differentiated into the
 114 continental crust and its mantle residue, which we will call the “residual mantle” (RM), in order to distinguish it
 115 from the “depleted mantle” (DM) associated with the three reservoir Earth. We show that this residual mantle
 116 occupies more than 70% of the total mantle, and its incompatible trace element budget is only moderately depleted.

117 We use the following terms and symbols to describe the various terrestrial silicate “reservoirs” evaluated by
 118 our mass balances:

- 119 CC - Bulk continental crust;
- 120 PM - Primitive mantle (equal to BSE = Bulk Silicate Earth);
- 121 DM - Depleted mantle reservoir in a 3-reservoir Earth, the product of extraction of CC from PM; DM
 122 should be capable of generating MORB or MORB+OIB;
- 123 EER - Early-enriched reservoir, either permanently stored in the deep mantle or possibly lost by
 124 collisional/accretion erosion;
- 125 EDR - Early-depleted reservoir = mantle after removal of EER but prior to extraction of permanent
 126 continental crust;
- 127 RM - Residual mantle reservoir in a 4-reservoir Earth consisting of PM, EER, EDR, and CC. RM is
 128 formed by extraction of CC from EDR.

129



130

131

132

133

134

135

136

137

138

139

140

141

142

143

144

145

146

147

148

Fig. 1. Nb/U vs. Th for mid-ocean ridge basalts (MORB), oceanic basaltic plateaus, and ocean island basalts (OIB), using MOR segment averages of Gale et al. (2013), average continental crust (Rudnick & Gao, 2003), primitive mantle (McDonough & Sun, 1995), average values for arc front volcanoes (Turner & Langmuir, 2015), and subducting sediments (Plank, 2014). Thorium concentrations are used as a proxy for overall incompatible-element enrichment/depletion. The primitive mantle (McDonough & Sun, 1995) is shown with a reduced Nb value of 0.555 ppm, instead of the value of Nb = 0.658 recommended by McDonough and Sun (1995). The reduced Nb is chosen to account for the loss of Nb from the bulk silicate Earth compared to chondrites (discussed in the section on reassessment of the Nb-Ta-Th-U relationships in oceanic basalts). The data for oceanic plateaus and OIBs were compiled from the GEOROC database (georoc.mpch-mainz.gwdg.de/), and filtered for evidence for U alteration using Th/U ratios (discussed in Supporting Information). The blue and red lines are regression curves for MORB and OIB data, respectively.

2. Data assessment

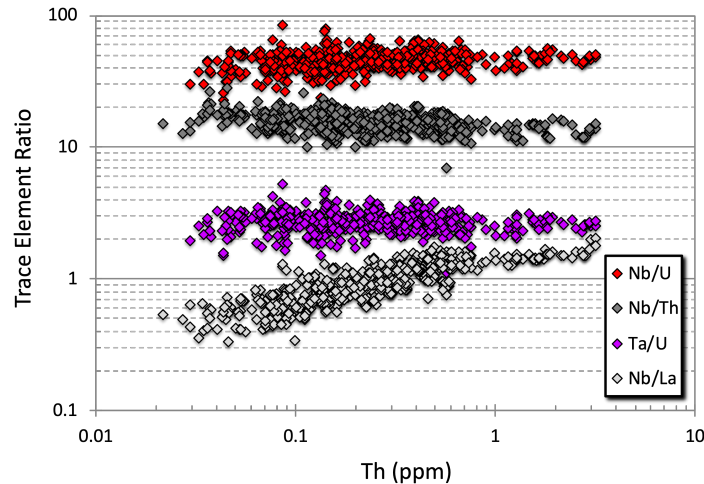
2.1. Reassessment of the Nb-Ta-Th-U relationships in oceanic basalts

Figure 1 is an update of Figure 1 of Hofmann et al. (1986) that showed Nb/U versus Nb concentrations. It illustrates the relationship of Nb/U between global MORB (Gale et al. 2013), a new compilation of OIB data (Supporting Information Table S1), the continental average of Rudnick and Gao (2003), arc front volcano averages

149 of Turner et al. (2015), subducting sediment averages of Plank (2014), and the primitive mantle value of
150 McDonough and Sun (1995). Thorium concentrations are used as proxies for overall incompatible-element
151 enrichment/depletion. Th in the abscissa rather than Nb avoids using the same variable in both coordinates, a
152 potential problem pointed out by Sims and DePaolo (1997). The original version in Hofmann et al. (1986) was based
153 on only 30 MORB samples and 41 individual OIB samples from 12 ocean island groups. In contrast, Figure 1
154 represents 260 global MOR segment averages, excluding segments from back arc basins, presented by Gale et al.
155 (2013), in addition to 30 OIB averages representing individual hotspots and seamount chains, as well as 7 oceanic
156 plateau averages, encompassing a total of nearly 4000 rock samples. A truly global assessment of Nb/U of OIBs is
157 still problematic, partly because there is no obvious way to obtain a globally representative sampling of OIBs and
158 their sources. In addition, many U data of OIBs are seriously compromised by alteration. The latter problem can be
159 recognized, and to some extent corrected for, by comparing the Nb/U ratios with Th/U ratios of the same samples.
160 Given the observation that all fresh OIBs have Th/U ratios between 3 and 5, close to the chondritic value of Th/U =
161 3.8, this has been used to screen most of the data (except those from historical eruptions; see Table S1). Preference
162 has therefore been given to historical eruptions, where fresh samples are readily available. Finally, oversampling of
163 individual OIB can be avoided by using single-volcano or single hotspot averages. The data plotted in Figure 1
164 represent the authors' best effort to provide a representative sampling of OIB data. They include several oceanic
165 plateaus, as well as several EM-type hotspots, which show slightly lower-than-average Nb/U ratios, consistent with
166 the presence of some continent-derived material in their sources. Remarkably, the mean Nb/U ratio of all these
167 OIBs, hotspots, volcanoes, and plateaus is $Nb/U = 47.0 \pm 6.6$ (1 std. dev.), which is indistinguishable from the
168 MORB average of $Nb/U = 46.1 \pm 9.2$ (Gale et al. 2013), as well as the value found by Hofmann et al. (1986) of 47
169 ± 10 . Our assessment of the similarity in Nb/U between MORB and OIBs is further substantiated by a plot of Nb/Th
170 vs. Th (Fig. S1), which shows the same relationships but is not significantly affected by sample alteration.

171 In order to use a trace element ratio (instead of an isotope ratio) of basalts to characterize their source
172 compositions, one needs to demonstrate that its value is independent of the degree of melting and therefore equal to
173 the source ratio (Hofmann et al., 1986). Trace element ratios that meet this requirement are independent of absolute
174 enrichment of the absolute concentrations of their incompatible elements, such as Th, are called "canonical." Figure
175 2 displays Nb/U, Nb/Th, Ta/U, and Nb/La as functions of the Th concentrations in the set of 583 MORB glasses
176 analyzed by Jenner and O'Neill (2012a). This shows that, at least for MORB samples, Nb/U and Ta/U ratios do not
177 significantly change, whereas Nb/Th decreases slightly as the Th concentration increases by a factor of about 100.
178 By contrast, the Nb/La ratio increases systematically by roughly a factor of three over the same Th range. Thus,
179 Nb/U and Ta/U appear to be suitable "canonical" ratios, and Nb/Th is nearly canonical, but Nb/La is not canonical.

180



181
 182 Fig. 2. Nb/U, Ta/U, Nb/Th, and Nb/La versus Th concentrations in about 600 MORB glasses. Data are
 183 from Jenner and O'Neill (2012a). This illustrates the essential requirements for selecting “canonical” trace
 184 element ratios: they must remain essentially constant and independent of source/melt depletion or
 185 enrichment in mantle-derived basalts. Nb/U and Ta/U meet this requirement nearly perfectly, whereas
 186 Nb/Th decreases slightly as a function of increasing Th. All three of these ratios are useful tracers of source
 187 composition. In contrast, Nb/La increases by about a factor of three as Th increases by two orders of
 188 magnitude. Thus, Nb/La is not a reliable tracer of source composition and should not be used as a
 189 “canonical ratio.”

190
 191 Sims and DePaolo (1997) pointed out that log (a) versus log (b) plots provide a statistically more rigorous
 192 assessment than the log (a)/(b) vs log (a) plot used by Hofmann et al. (1986). Figure S2 shows such logU-logNb and
 193 logU-logTa plots for three published datasets of global MORBs by Arevalo and McDonough, (2010), Jenner and
 194 O'Neill, (2012a), and Gale et al. (2013) to evaluate the slopes of these plots. Ideally, if these ratios were constant
 195 over the entire range of absolute concentrations, the slopes of such correlations would equal 1.0. The actual slopes
 196 for all three datasets are slightly lower than 1.0 for logU vs. logNb, and slightly greater than 1.0 for log U vs. logTa.
 197 Figure S3 shows how these slopes vary systematically for a larger range of trace element ratios, involving Ba, Th, U,
 198 Nb, Ta, K, and La. These systematic variations in slopes of log-log plots can be translated into a sequence of
 199 increasing compatibility of Ba < Th < Nb < U < Ta < K < La, based on global MORB data. We can also conclude
 200 from this analysis that both Nb/U and Ta/U closely approach the ideal “canonical” (i.e. invariant) status, but a ratio
 201 of uranium with an element with properties intermediate between Nb and Ta would be needed to form a perfectly
 202 invariant ratio.

203 Arevalo and McDonough (2010) raised the issue whether an element pair can be used for a “canonical”
 204 ratio that also characterizes its source, if its log-log slope deviates slightly from 1.0. To address this issue, we use a

205 simple bracketing method. We calculate the size and composition of the source reservoir first for Nb/U, which
 206 consistently yields slopes slightly less than 1.0 in the log-log plots of Figure S2, and then for Ta/U, which
 207 consistently yields slopes slightly greater than 1.0. It turns out that the results are nearly indistinguishable, thus
 208 validating both ratios as being adequately “canonical” for the purpose at hand.

209 Table S3 shows the mean Nb/U, Ta/U, and Nb/Th ratios obtained from the three sets of MORB data. We
 210 note that the three data sets agree remarkably well. The most important exception is the value of Ta/U = 2.75 for
 211 average MORB by Jenner and O’Neill (2012a) which is significantly lower than the values of 2.91 and 3.09 given
 212 by Arevalo and McDonough (2010) and by Gale et al. (2013), respectively. This difference appears to be largely the
 213 result of an interlaboratory bias, because Jenner and O’Neill (2012b) report a Ta value for BCR-2G that is 6.7%
 214 lower than the preferred GeoReM value for this reference material (<http://georem.mpch-mainz.gwdg.de>). For the
 215 purpose of this paper, we will use values obtained by Gale et al. (2013).

216

217 **2.2. Bulk-Silicate Earth Nb/U and Ta/U ratios**

218 In this paper, we use Bulk Silicate Earth (BSE) values of Ta/U = 1.82 (McDonough and Sun, 1995) and
 219 Nb/U = 27.34, which is lower than McDonough and Sun’s recommended value of 32.4. These values correspond to
 220 a BSE value of Nb/Ta = 15.5 instead of Nb/Ta = 17.78 (McDonough and Sun, 1995). This reduction of BSE
 221 niobium has a relatively minor effect on our quantitative results, but it is indicated by data; for example, nearly all
 222 known terrestrial silicate samples have lower-than-chondritic Nb/Ta, most likely due to incorporation of Nb in
 223 Earth’s core (e.g Huang et al. 2020; see also Supporting Information).

224

225 **3. Testing the 3-reservoir silicate Earth model by mass balance**

226 **3.1. Equations and input parameters 3 Data, or a descriptive heading about data**

227 Following Davies (1981), the mass balance in a simple, three-reservoir silicate Earth consisting of the
 228 continental crust, the complementary depleted mantle reservoir, and a “left-over” primitive mantle reservoir, yields
 229 X_{dm} , the mass fraction of the depleted mantle reservoir

$$230 \quad X_{dm} = \frac{X_{cc} C_{cc} (R_{dm} - R_{cc})}{C_{pm} (R_{dm} - R_{pm})} - X_{cc} \quad (1)$$

231 where X is the mass fraction of a given reservoir, R is an isotopic or canonical chemical abundance ratio, C is the
 232 concentration of the chemical element in the denominator of R , and the subscripts cc , pm , and dm identify the three
 233 reservoirs continental crust, primitive mantle, and depleted mantle, respectively.

234 The concentration of the element in the denominator of ratio R is given by:

235

$$236 \quad C_{dm} = \frac{C_{pm} (X_{dm} + X_{cc}) - X_{cc} C_{cc}}{X_{dm}} \quad (2)$$

237

238 For the readers’ convenience, the derivation of equation (1) and (2) is given in the Supporting Information.

239 Here we initially specify (Nb/U) and (Ta/U) for R , in order to solve equations (1) and (2). Subsequently, we
 240 repeat this calculation using $\varepsilon(Nd)$ for R , in order to compare the results. The input parameters for the primitive
 241 reservoir pm are taken from McDonough and Sun (1995), except for the value of Nb, which we reduce from 0.658
 242 ppm to 0.555 ppm in order account for the Nb deficiency in the bulk silicate Earth (Section 2.3 and Supporting
 243 Information. The parameters for the continental crust U_{cc} , $(Nb/U)_{cc}$ and $(Ta/U)_{cc}$ are from Taylor and McLennan
 244 (1985), Rudnick and Fountain (1995), Rudnick & Gao, (2003), McLennan et al. (2006), and Hacker et al. (2015).
 245 These parameters are listed in Table S4. We note that the estimates for the crustal abundance of U in the above
 246 publications range from 0.91 to 1.4 ppm. Even higher values for the crustal U abundance can be found in the
 247 literature, but will not be considered here. We further note that the U value of = 0.91 ppm given by Taylor and
 248 McLennan (1985) was revised to U = 1.1 ppm by McLennan et al. (2006). A minimum of U = 1.1 ppm is also found
 249 in three of the five crustal models given by Hacker et al. (2015). The maximum value given by these authors is U =
 250 1.33 ppm, and this is nearly identical to the value of U = 1.3 ppm given by Rudnick and Gao (2003). We will use a
 251 range of crustal U = 1.1 to 1.3 ppm in the following calculations. Nb and Ta abundances of the bulk continental
 252 crust are less critical in the mass balance calculations. McLennan et al. (2006) and Rudnick and Gao (2003) give a
 253 value of Nb = 8 ppm, whereas the five models of Hacker et al. (2015) yield a range of Nb = 7.4 to 8.8 ppm. In
 254 contrast, the estimates of the above authors for Ta are more variable, ranging from Ta = 0.52 to 0.8 ppm. These
 255 variations in Nb and Ta estimates of the continental crust are the cause of the minor scatter in the mass balance
 256 results in Figure 3.

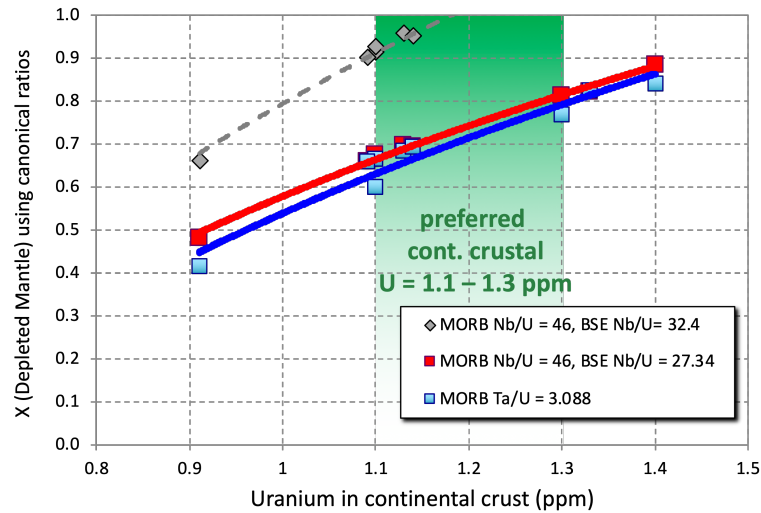
257 The initial assumption of a very simple, three-reservoir silicate Earth represents an important
 258 simplification. Indeed, such a model harks back to the time when Earth's mantle was widely thought to consist of a
 259 depleted upper and a primitive lower mantle, as discussed in the Introduction. In its simplest form, this model has
 260 largely been laid to rest by the findings of seismic tomography and geochemistry. We will use it as a starting point
 261 in our evaluation of the mantle reservoir involved in forming the continental crust. As already noted, it will be seen
 262 from our reevaluation of the analogous mass balance using Nd isotopes that this model is not adequate for
 263 describing Earth's silicate interior, and this result will lead us to postulate the existence of an additional, enriched,
 264 and now hidden or lost, reservoir.

265

266 **3.2. Preliminary evaluation of the mass fraction of Depleted Mantle (DM) based on** 267 **canonical ratios**

268 Figure 3 shows the mass of the residual mantle, using equation (4) with our preferred input parameters
 269 $(Nb/U)_{BSE} = (Nb/U)_{pm} = 27.34$, $(Ta/U)_{bse} = (Ta/U)_{pm} = 1.82$, $(Nb/U)_{dm} = 46$, $(Ta/U)_{dm} = 3.09$, crustal Nb/U and Ta/U
 270 values given in Table S4, and showing a preferred range of crustal uranium contents between 1.1 and 1.3 ppm. Thus,
 271 "bracketing" the calculation with two nearly perfectly canonical ratios leads to virtually identical results, showing a
 272 mass fraction of DM ranging from $X_{dm} = 0.6$ to 0.8. In contrast, the gray dashed line based on a BSE with a strictly
 273 chondritic Nb/U ratio would require a DM mass fraction of $X_{dm} = 0.9$ to impossible values of $X_{dm} > 1.0$. Overall,
 274 Figure 3 demonstrates that, for the simple three-reservoir model, the mass of DM amounts to more than 60 percent
 275 of the total mantle, assuming a range of crustal U values of 1.1 to 1.3 ppm as discussed above, far exceeding the

276 mass fraction of the upper mantle above 660 km (about 30% by mass) traditionally inferred in the literature on the
 277 basis of Nd isotopes.



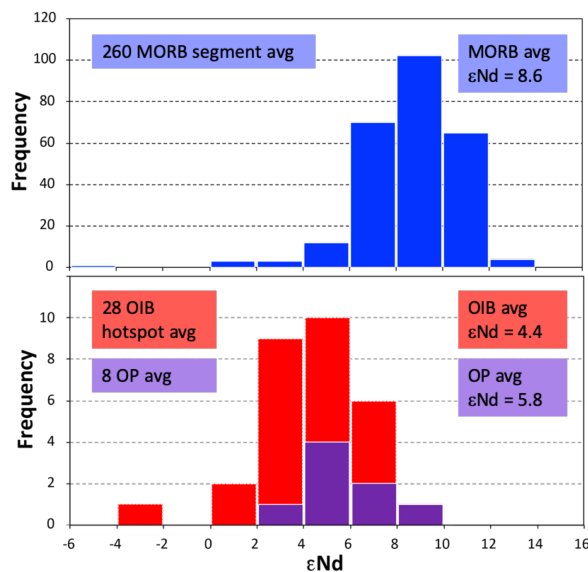
278
 279 Fig. 3. Mass fraction of depleted mantle, X_{dm} , based on the canonical ratios Nb/U and Ta/U in a three-
 280 reservoir Earth model. X_{dm} is calculated from equ. (1) and a MORB average of Nb/U = 46 given by Gale et
 281 al. (2013) and Jenner and O'Neill (2012a), as well as Ta/U = 3.088 from Gale et al. (2013) as the R_{dm}
 282 parameters. The resulting value of X_{dm} depends significantly on the bulk U content assumed for the
 283 continental crust, U_{cc} . We use a variety of published crustal U estimates taken from Rudnick and Gao
 284 (2003), McLennan et al (2006), and Hacker et al. (2015), all within our “preferred range” of $U_{cc} = 1.1$ to 1.3
 285 ppm, indicated by the green shaded region. The Nb/U and Ta/U-based results are in good agreement, if the
 286 reduced bulk silicate-Earth Nb value of 0.555 is used, yielding Nb/U 27.34 and Nb/Ta = 15.00 for the BSE
 287 (see text). By contrast, the dashed curve, using an uncorrected BSE abundance for Nb, displays significant
 288 disagreement with the Ta/U-based curve. The data points defining the red, blue and dashed lines
 289 correspond to crustal estimates of U and Nb in the literature (Hacker et al., 2015; McLennan et al., 2006;
 290 Rudnick & Fountain, 1995; Rudnick & Gao, 2003; Taylor & McLennan, 1985) listed in Table S4, where
 291 the different estimates mostly represent different assumptions about the lower crust composition.

292

293 3.3. Comparison with mass fraction of the Depleted Mantle (DM) based on Nd isotopes.

294 In order to compare the mass balances based on Nb/U or Ta/U with those based on Nd isotopes, we cannot
 295 simply use the Nd isotope data of the depleted MORB reservoir, as was done in the earlier estimates based on Nd
 296 isotopes, or even one based on all MORB data. This is because the (Nb,Ta)/U ratios shown in Figure 1 demonstrate
 297 clearly that the sources of both MORB and OIB must be included in this calculation. Thus, to validate such a

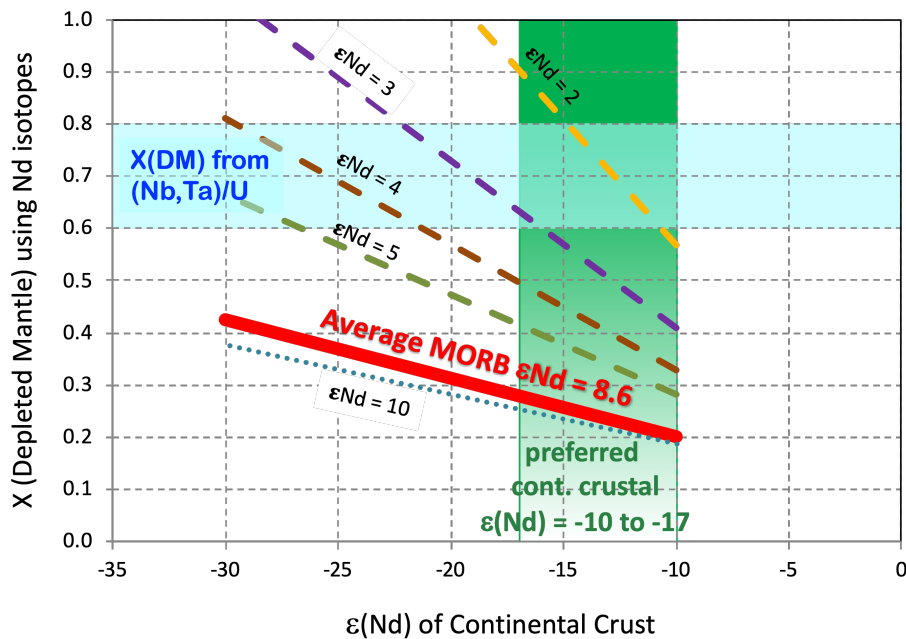
298 comparison, we must attempt to include the Nd isotopic composition of the OIB source(s) as well, even though
 299 MORB and OIB show systematic isotopic differences. Figure 4a shows frequency plots for MORB data from Gale
 300 et al. (2013), which we regard as representing the isotopic composition of the global asthenosphere. Figure 4b shows
 301 the results of our compilation of average compositions for ocean islands and oceanic plateaus (Table S5). Taken
 302 together, these data should represent the entire mantle sampled by volcanism. Unfortunately, it is uncertain how
 303 these two families of mantle-derived basalts should be weighted to obtain a representative average for the entire
 304 mantle. Therefore, we once again use a bracketing approach by making two extreme assumptions: (1) the
 305 composition of DM is given by the MORB average of $\epsilon(\text{Nd}) = 8.6$; (2) DM is represented by the averages of OIB
 306 $\epsilon(\text{Nd}) = 4.4$ and oceanic plateaus of $\epsilon(\text{Nd}) = 5.8$. We assume that the true value lies somewhere between these
 307 extremes.



308
 309 Fig. 4. Histogram of $\epsilon(\text{Nd})$ values of mid-ocean ridge segment averages (Gale et al., 2013) and a new
 310 compilation of oceanic hotspot averages (Table S5). The OIB data for the 37 hotspots selected for this
 311 compilation are mostly those listed by Sleep (1990) and a few additional ones for which adequate $\epsilon(\text{Nd})$
 312 data exist. In addition, we compiled data for several oceanic plateaus. Each hotspot average represents the
 313 average value of individual volcano averages belonging to a given hotspot. The particular volcanoes
 314 selected are in some cases, such as Iceland, incomplete and somewhat arbitrary; they are largely governed
 315 by the availability of data. The hotspot data show a mean value of $\epsilon(\text{Nd}) = 4.4 \pm 2.3$ (1 std deviation),
 316 corresponding to a standard error of ± 0.4 for 28 hotspots. The Pacific oceanic plateaus yield a mean value
 317 of $\epsilon(\text{Nd}) = 5.8$. We also note that the hotspot averages have not been weighted for the plume flux given by
 318 Sleep (1990). We suggest that, given the existing sampling of hotspots, a perfectly representative
 319 distribution of hotspot isotopic compositions is probably not possible at the present time, but the data are
 320 adequate for our evaluation.

321

322 Figure 5 shows the results of the Nd-isotope-based mass balance calculations, using equation (1) for $\epsilon(\text{Nd})$
 323 values ranging from 8.6 (average MORB) down to $\epsilon(\text{Nd}) = 2$ (a value even lower than average OIBs). For the
 324 continental crust, we choose a range of $\epsilon(\text{Nd}) = -10$ to -17 , which includes the estimates given by Goldstein et al.
 325 (1984), Goldstein and Jacobsen (1988), Rudnick (1990), and Chauvel et al. (2014). Figure 5 shows that the lowest
 326 possible mass fraction of the depleted mantle, $X_{\text{dm}} = 0.2$, is obtained by the combination of $\epsilon(\text{Nd}) = -10$ for the
 327 continental crust and $\epsilon(\text{Nd}) = +8.6$ for DM. The maximum value, obtained by the combination of $\epsilon(\text{Nd}) = -17$ for the
 328 crust and $+4.0$ for the depleted mantle, respectively, is $X_{\text{dm}} = 0.5$. Thus, there is no overlap between this range (X_{dm}
 329 $= 0.2$ to 0.5) and the range obtained by the equivalent calculation based on Nb/U or Ta/U, namely $X_{\text{dm}} = 0.6$ to 0.8 .
 330 We conclude that the inclusion of the OIB source reservoir is unable to reconcile the two independent mass balance
 331 calculations of a 3-reservoir silicate Earth, thus ruling out the simple 3-reservoir model for the Earth.



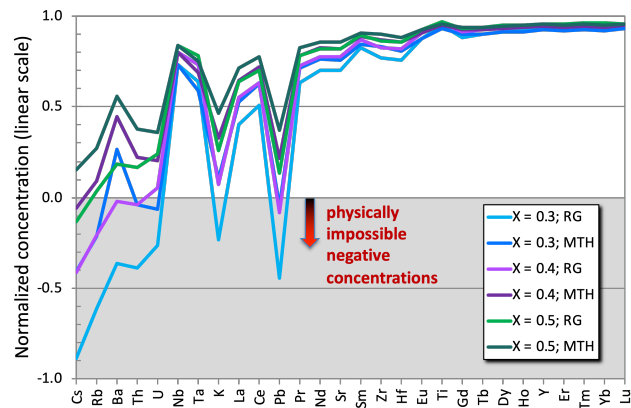
332
 333 Fig. 5. Mass fraction of DM, X_{dm} , defined as the residue of continent extraction in a conventional three-
 334 reservoir Earth model (continental crust, depleted mantle, primitive mantle) based on Nd isotope ratios.
 335 Mass balance results are shown for a range of possible $\epsilon(\text{Nd})$ values of mantle and average continental
 336 crust. The range of acceptable average continental values, $\epsilon(\text{Nd}) = -10$ to -17 is taken from the literature
 337 (see text) and is indicated by the green shaded region. The $\epsilon(\text{Nd})$ values assumed for DM range between the
 338 average MORB value ($\epsilon(\text{Nd}) = 8.6$) to lower, less depleted values that might represent an integrated DM
 339 reservoir incorporating MORB+OIB sources, $\epsilon(\text{Nd}) = 5, 4, 3, 2$. If DM occupies a mass fraction of $= 0.6$ to
 340 0.8 (blue shaded region, taken from the Nb/U-based mass balance shown in Fig. 3), the $\epsilon(\text{Nd})$ value of such

341 an integrated MORB+OIB reservoir would have to be unrealistically low ($\epsilon(\text{Nd}) \leq 3.5$). This is inconsistent
 342 with observed $\epsilon(\text{Nd})$ values of average MORB (8.6), average OIB (4.4), and oceanic plateaus (5.8); see also
 343 Fig. 6

344

345 We further examine this result by calculating the composition of DM from equation (2) using its mass
 346 fraction and the estimated composition of the continental crust by Rudnick and Gao (2003) – RG, and McLennan et
 347 al. (2006) – MTH (Fig. 6). A DM mass fraction as small as $X_{\text{dm}} = 0.3$ results in several of the most highly
 348 incompatible elements in DM to have negative concentrations, which is of course physically impossible, providing
 349 independent confirmation that the present-day continental crust was extracted from much more of the mantle than
 350 just its upper part.

351 Another awkward feature of the conventional small volume, highly depleted DM is examined in Figure S4,
 352 which is an iteration of the partial melting model of Workman and Hart (2005), who calculated a melt fraction of 6%
 353 to generate an average MORB composition from their depleted mantle. By simply replacing the so-called “N-
 354 MORB” average used by Workman and Hart (2005) by the modern, more representative ALLMORB average given
 355 by Gale et al. (2013), Figure S4 shows that a melt fraction of 3% would be required to generate ALLMORB from
 356 such a Workman-Hart-type DM reservoir. Such a low melt fraction is at odds with independent estimates of MORB
 357 melting, which range from 8 to 20% melt fractions (Klein & Langmuir, 1987). Finally, our results reinforce
 358 Campbell’s (2002) conclusion, based on partial melting modeling, that extraction of the continental crust contributes
 359 only a portion of the observed change in Sm/Nd and consequently $\epsilon(\text{Nd})$ of the residual mantle.



360

361 Fig. 6. Three-reservoir mass balance based on MORB $\epsilon(\text{Nd})$ yields impossible results: DM compositions
 362 (PM-normalized) calculated from the mass balance equation (2), for conventional, $\epsilon(\text{Nd})$ -based mantle
 363 models that limit the mass fraction X_{dm} of the depleted mantle to less than 50% of the total mantle. The
 364 case of $X_{\text{dm}} = 0.3$ corresponds to a DM reservoir restricted to the upper 660 km of the mantle. Results are
 365 shown for $X_{\text{dm}} = 0.3, 0.4, \text{ and } 0.5$, and for continental crustal compositions given by Rudnick and Gao

(2003) – RG, and McLennan et al. (2006) - MTH. Especially for the case of $X_{dm} = 0.3$, several of the most highly incompatible elements, including Th and U, end up with (physically impossible) negative concentrations in the DM for both bulk crustal compositions. This provides additional, independent evidence that conventional, $\epsilon(\text{Nd})$ -derived continental crust-mantle mass balances are based on incorrect assumptions.

3.4. What causes the discrepancy between the two depleted mantle (DM) estimates?

Our mass balance based on $\epsilon(\text{Nd})$ explicitly included the OIB source reservoir(s), in addition to the traditionally used MORB source reservoir, to represent the DM complement of the continental crust. In spite of its inclusion in the mass balance, the OIB source reservoir(s) are not sufficiently enriched to yield a mass balance that is consistent with the (Nb,Ta)/U-based mass balance. This means that there must be at least one additional enriched (i.e. low- $\epsilon(\text{Nd})$) reservoir to achieve an overall mass balance for the bulk silicate Earth, assuming that BSE possesses chondritic $\epsilon(\text{Nd})$, Ta/U, and near-chondritic Nb/U values. Such an additional enriched reservoir may have been lost from the Earth by collisional erosion, as suggested e.g. by O'Neill and Palme (2008). Alternatively it may be hidden in the lowermost mantle in form of an EER (= early enriched reservoir), as proposed by Tolstikhin and Hofmann (2005) and Boyet and Carlson (2005). Below, we will further explore the option of an early-enriched reservoir. This will force us to expand the 3-reservoir BSE to a 4-reservoir BSE.

4. The four-reservoir silicate Earth

4.1 The hidden, early-enriched reservoir (EER) and the early-depleted reservoir (EDR)

We suggest that an early-enriched reservoir (EER) is generated by the formation and permanent sequestration of an early mafic crust. This EER is similar but not identical to the EER suggested by Boyet and Carlson (2005, 2006) on completely different grounds, namely their discovery of elevated, non-chondritic $^{142}\text{Nd}/^{144}\text{Nd}$ ratios of the (accessible) bulk silicate Earth (as represented by continental crust, MORB, and OIB). The composition of Boyet and Carlson's EDR (Early Depleted Reservoir) and its complementary EER were estimated in part by a mass balance involving a Depleted Mantle reservoir derived from a crust-mantle differentiation model similar to that developed by Workman and Hart (2005). This model, in turn, involved the composition of the present-day continental crust (which did not exist at the time of EER sequestration), and this imparted a substantial negative Nb anomaly on the trace element pattern of the EDR of Boyet and Carlson (2005, 2006). We suggest that this anomaly is a result of adding the present-day continental crust to the modeled present-day MORB source, an approach that must now be abandoned because we have shown that the present-day MORB source cannot be the simple complement of the present-day continental crust (more details are in Supporting Information B).

Here we model EER using a simple batch melting process that generates a now-lost early mafic crust. We sequester (by subduction or loss to space) a small amount of it, leaving behind a large, moderately depleted EDR, which occupies the remainder of the mantle. The EDR then differentiates into the continental crust and the depleted mantle (MORB + OIB) reservoir, which we call "Residual Mantle" (RM) for the 4-reservoir model to distinguish it

403 from the 3-reservoir model, in which the residue of the continental crust was referred to as “Depleted Mantle” (DM).
 404 Because of the permanent sequestration of the EER, we can reformulate equation (1) for the subsequent
 405 differentiation of EDR into CC (continental crust), Residual Mantle (RM), incorporating both MORB and OIB
 406 sources, and a “left-over” amount of EDR. This reformulation amounts to a modified 3-reservoir system (plus an
 407 isolated EER) and the reformulated equation (1) will be labeled equations (3) and (4) as discussed below:

408 The two new balance equations, one formulated for (Nb/U), the other for $\epsilon(\text{Nd})$, can be solved to find a
 409 common (identical) value of the mass fraction of the residual mantle.

410

$$411 \quad X_{RM} = \frac{X_{CC} Nd_{CC} (\epsilon_{RM} - \epsilon_{CC})}{Nd_{EDR} (\epsilon_{RM} - \epsilon_{EDR})} - X_{CC} \quad (3)$$

412

$$413 \quad X_{RM} = \frac{X_{CC} U_{CC} (Nb/U_{RM} - Nb/U_{CC})}{U_{EDR} (Nb/U_{RM} - Nb/U_{EDR})} - X_{CC} \quad (4)$$

414

415 If the EER is permanently lost from Earth by collisional erosion (O’Neill and Palme, 2008), the mass
 416 fractions calculated from equations (3) and (4) will equal the actual mass fractions in the silicate Earth. If, on the
 417 other hand, EER remains buried in the mantle, these mass fractions will have to be reduced by a factor of $(1 - X_{eer})$
 418 in order to correspond to the actual mass fractions of the total silicate Earth. There are four unknowns, X_{rm} , Nd_{edr} , ϵ_{edr} ,
 419 U_{edr} , in equations (3) and (4), with ϵ short for $\epsilon(\text{Nd})$. However, using a simple model of partial melt segregation for
 420 generating the EDR, we can replace three of these variables by a single one, X_{eer} . This is because for a given melt
 421 fraction F and age of the silicate Earth, say $F = 0.1$ and 4.57 Ga, the melt segregation model uniquely determines
 422 Nd_{edr} , ϵ_{edr} , and U_{edr} , as a function of the sequestered melt fraction, namely the Early Enriched Reservoir, X_{eer} . In this
 423 approach ϵ_{edr} is calculated from the resulting Sm_{edr} combined with Nd_{edr} , and using the radioactive decay equation to
 424 determine the present-day $^{147}\text{Sm}/^{144}\text{Nd}$ ratio. We thus have only two variables, X_{EER} and X_{RM} to solve the two
 425 equations (3) and (4), as for each value of X_{EER} there is a specific value of Nd_{EDR} , U_{EDR} and ϵ_{EDR} , which is
 426 determined by the equations for partial melting and radioactive decay, respectively. The solution is then given by the
 427 intersections of the two functions (3) and (4), as shown in Fig. S5.

428 We solved this system of equations numerically, using partitioning data for spinel lherzolite given by
 429 Salters and Stracke (2004). Specific values of these solutions for X_{rm} , ϵ_{edr} , X_{eer} are given in Table S6. Figure 7
 430 shows the results for an assumed melt fraction of $F = 0.1$ to generate the now-lost early mafic crust. Figure 7a gives
 431 the range of mass fractions of RM as a function of its ϵ_{rm} value, covering the range of $\epsilon_{rm} = 4.5$ to 8.5 , that is, the
 432 possible mixtures of OIB and MORB averages discussed earlier. In order to explore the full range of solutions, we
 433 plot the results for the four possible combinations of the extreme values of the crustal composition estimates, $U_{CC} =$
 434 1.1 and 1.3 ppm, $\epsilon_{CC} = -10$ and -17 . The central red line shows the results for intermediate values, namely $\epsilon_{CC} = -12$
 435 and $U_{CC} = 1.2$ ppm for the continental crust. The important result is that the possible mass fractions of residual
 436 mantle range from about 72% to nearly 100% of the mantle (except for the 1 to 3% occupied by the EER). Figure 7b
 437 shows the corresponding mass fractions of the sequestered EER, which range from about 1-3% of the mantle. Figure

438 7c shows the respective ϵ_{EDR} values. In both cases, using a crustal U value of 1.3 ppm (Rudnick & Gao, 2003), the
 439 range of ϵ_{EDR} and X_{EER} is “cut off” by the fact that $X(RM)$ has reached or exceeded 98% of the mantle (Fig. 7a), so
 440 that the EDR has been completely used up to make CC and RM.

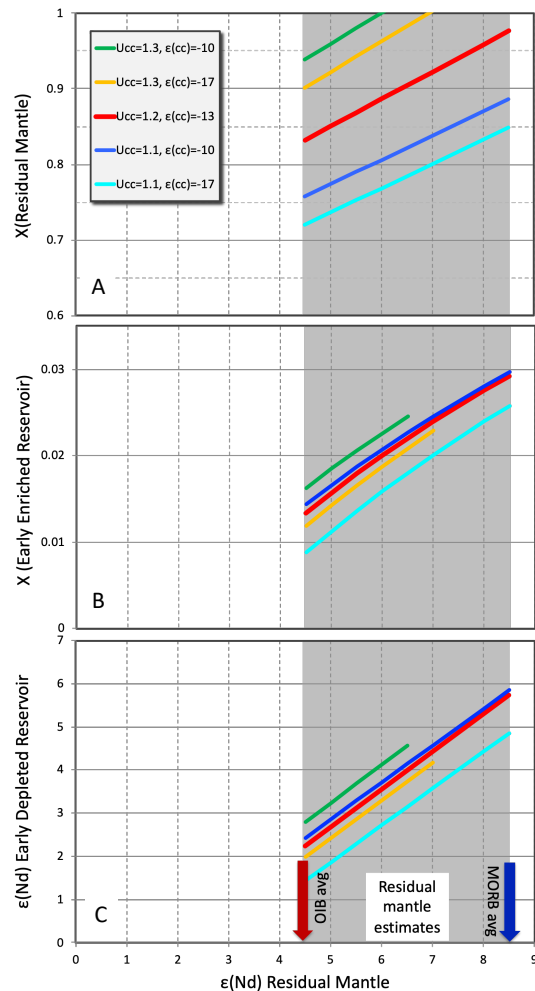
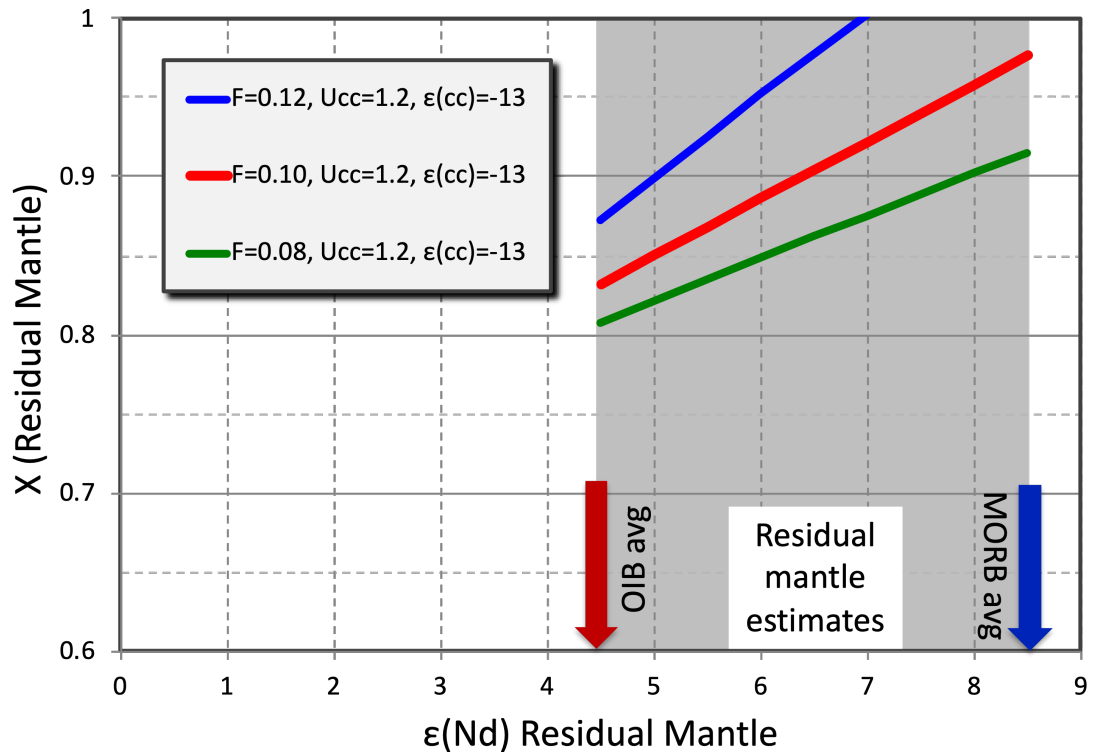


Fig. 7

441
 442 Fig. 7. Specific solutions for the new 4-reservoir models described by equations (3) and (4), all plotted
 443 against the full range of $\epsilon(\text{Nd})_{\text{rm}}$ values ($\epsilon(\text{Nd}) = 4.5$ to 8.5) of the combined MORB-plus-OIB source
 444 reservoir. Models are calculated for an EER formed by a (batch) melt fraction of $F = 0.10$, using partition
 445 coefficients for spinel lherzolite from Salters and Stracke (2004). (7a) Mass fraction of residual mantle,
 446 X_{rm} versus $\epsilon(\text{Nd})_{\text{rm}}$ for crustal compositions with $U_{\text{cc}} = 1.1$ and 1.3 ppm, and $\epsilon(\text{Nd})_{\text{cc}} = -10$ and -17 ,
 447 representing the extreme range of assumed crustal compositions. (7b) Mass fraction of the Early Enriched
 448 Reservoir, X_{eer} , for the same range of crustal compositions. (7c) $\epsilon(\text{Nd})_{\text{edr}}$ for the same range of crustal
 449 compositions.

450

451 Figure 8 shows the effect of varying the melt fraction that generates the now-lost early mafic crust and thus
 452 the EER, using alternative melt fractions of $F = 0.08$ and 0.12 . For clarity, we restrict this to the case of an
 453 intermediate crustal composition of $U_{cc} = 1.2$ ppm and $\epsilon_{Nd} = -12$. We infer from these results that the scope for
 454 varying the melt fraction generating EER is limited. Higher melt fractions are limited by the fact that X_{rm} cannot
 455 exceed $(BSE - X_{eer})$, about 0.98 . Smaller melt fractions cause the size of $X(RM)$ to be only slightly lower, but would
 456 require the generation of more and more alkaline melts, such as are not found, for example, in Archean greenstones.
 457 All solutions yield $X_{RM} > 70\%$ of the total mantle, and in the more U-rich crustal models, especially the crustal U
 458 estimate of Rudnick and Gao (2003), the residual reservoir may occupy more than 90% of the mantle. Nevertheless,
 459 most models leave room for a significant amount of EDR in the mantle.



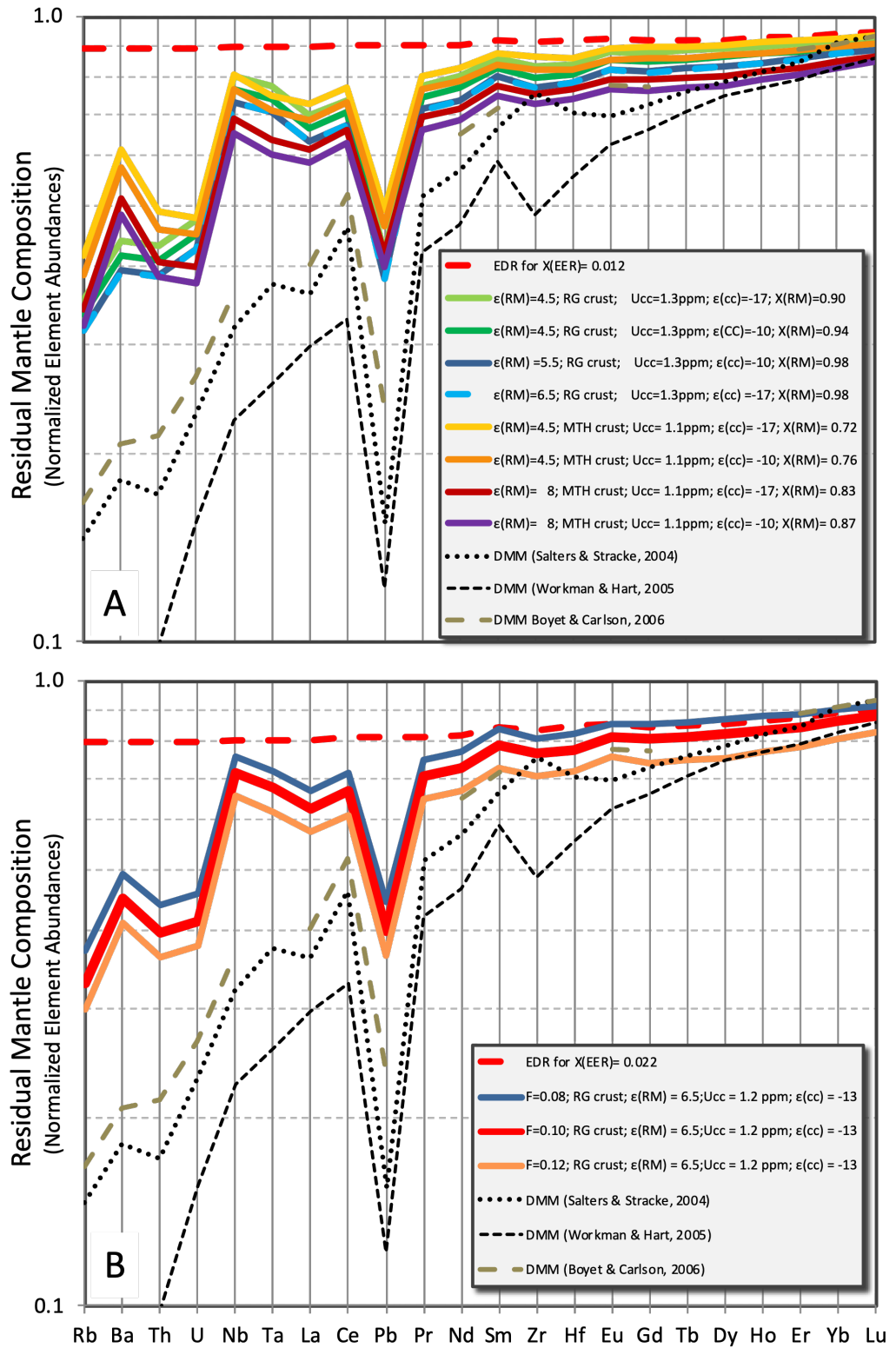
460
 461 Fig. 8. Solutions of equations (3) and (4) for three different melt fractions forming EER, $F = 0.08, 0.10,$ and
 462 0.12 . The crustal composition assumed here is an intermediate value of the one used in Figure 7, namely
 463 $U_{cc} = 1.2$ ppm, and $\epsilon(Nd)_{cc} = -13$.

464
 465

466 With the above results, in particular the values for $X(RM)$ given in Figure 7a, we can now calculate the
 467 trace element abundances of RM, using a modified version of equation (2), in which the Primitive Mantle is
 468 replaced by the EDR:

$$469 \quad C_{RM} = \frac{C_{EDR} (X_{RM} + X_{CC}) - X_{CC} C_{CC}}{X_{RM}} \quad (5)$$

470
 471 *Figure 9* shows the element abundances of the residual mantle for the same range of crustal compositions
 472 used further above, and for a range of choices for the $\epsilon(Nd)$ composition of the residual mantle. In order to cover the
 473 full range of solutions, Fig. 9a gives the Residual Mantle abundances for an Early Enriched Reservoir generated by a
 474 melt fraction of $F = 0.10$ and the extreme values of the continental crust, $\epsilon(Nd) = -10$ and -17 , and uranium
 475 concentrations of $U = 1.1$ and 1.3 ppm and extreme values of $\epsilon(Nd)$ of the Residual Mantle of 4.5 and 8.0 . In cases
 476 where the calculated total mass fraction of the Residual Mantle exceeds $X_m = 0.98$, an appropriately lower value of
 477 $\epsilon(RM)$ is used. Figure 9b illustrates the effect of varying the initial melt fraction of EER. We suggest that the melt
 478 fraction cannot be arbitrarily increased to even higher values, because this would require the sequestration of
 479 seemingly unreasonably large EERs. At $F = 0.12$, the size of the EER would already be quite large, $X(EER) = 2.5$ to
 480 over 4%.



482 Fig. 9a. Normalized incompatible-element plots for the models shown in Figure 7. Shown are the Residual
483 Mantle compositions corresponding to two crustal compositions of Rudnick and Gao (2003) and McLennan
484 et al. (2006), labeled RG crust and MTH crust, respectively. Normalizing concentrations are from
485 McDonough and Sun (1995).

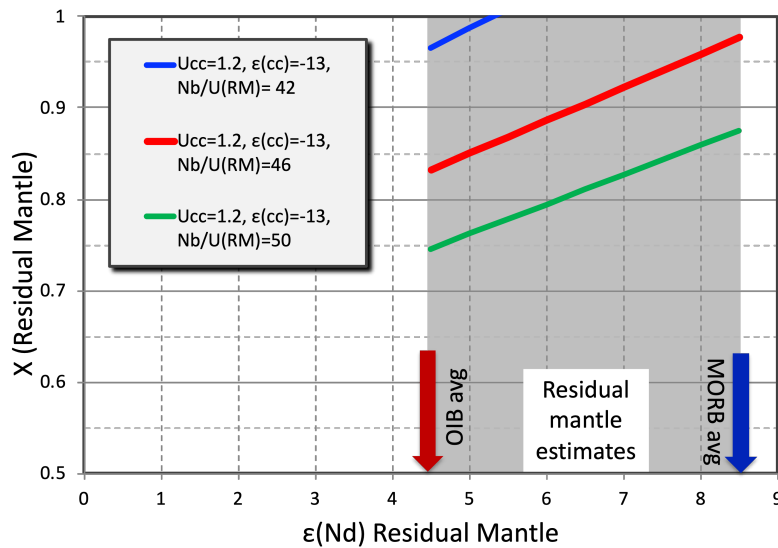
486 Fig. 9b. Normalized incompatible-element plots for the models shown in Figure 8. Shown are the Residual
487 Mantle compositions corresponding to the averages of the two crustal concentration values of Rudnick and
488 Gao (2003) and McLennan et al. (2006). The 3 solid lines correspond to $F = 0.08, 0.10,$ and 0.12 as in Fig.
489 8. Also shown is the corresponding composition of Early Depleted Reservoir, EDR, for the case of $F = 0.1$.
490 For comparison, we also show the abundance patterns of the traditional Depleted Mantle (DMM) models of
491 Salters and Stracke (2004). Workman and Hart (2005) and Boyet and Carlson (2006).

492
493

494 The resulting Th and U abundances of the residual mantle are all significantly higher than the three
495 published DMM estimates, even though the corresponding X_{RM} values range from about 70% to nearly 100% of the
496 total mantle. The seemingly strange positive Ba anomalies in the RM trace element patterns using the crustal
497 abundances of McLennan et al. (2006), is the result, possibly an artifact, of their relatively low Ba abundances
498 (250ppm versus 540 ppm for the Rudnick-Gao crust) of their crustal model.

499 For comparison, we also show the abundance patterns of the traditional Depleted Mantle (DMM) models of
500 Salters and Stracke (2004). Workman and Hart (2005) and Boyet and Carlson (2006). Thus, the actual Residual
501 Mantle that is chemically complementary to the continental crust is far less severely depleted in highly incompatible
502 elements than had been inferred by previous evaluations of the DM composition. In particular, the heat production
503 (as given by the Th and U abundances) of the Residual Mantle is now seen to be two to five times higher than
504 previously thought.

505 In order to assess the question of how sensitive our results are to the precise value of the Nb/U and Ta/U
506 ratios of the Residual Mantle, we compare results for Nb/U = 42, 46, and 50 for a Residual Mantle generated by
507 crustal values of $U_{cc} = 1.2$ ppm and $\epsilon(cc) = -13$ (Fig. 10). Thus, if the Nb/U ratio of the Residual Mantle were as
508 high as 50, its mass fraction would be substantially reduced, especially at the lowest value of $\epsilon(RM) = 4.5$, but it
509 would still exceed 70% of the total mantle.



510

511 Fig. 10. Same as Fig. 8, but assuming three values of Nb/U for the Residual Mantle, Nb/U = 42, 46, and 50.

512 This explores how sensitive the results are to the precise value of $(\text{Nb}/\text{U})_{\text{rm}}$ used for the mass balance

513 calculation. Even though this range is much larger than the standard errors of both the MORB and the OIB

514 data, this shows that the minimum mass fraction of the Residual Mantle, X_{rm} , is still greater than 70%.

515

516 The preceding discussion has shown that, depending on the specific assumptions about the isotopic and
 517 elemental composition of the crust and the present-day mantle, a fairly wide range of solutions is possible for size
 518 and composition of Earth's residual mantle. What all of these solutions have in common though is that the mantle
 519 residue of the present-day continental crust fills at least 70%, and possibly nearly all of the mantle, and it is
 520 substantially less depleted in incompatible elements than previously thought. Table 1 gives the calculated
 521 composition for a residual mantle and continental crust that is compositionally intermediate between the more
 522 extreme values used in the preceding calculations. This gives the normalized "average" composition for a combined
 523 MORB-plus-OIB source mantle characterized by $\epsilon(\text{Nd}) = 6.5$, a melt fraction generating the Early Enriched
 524 Reservoir of $F = 0.10$, and a crustal composition that is an average between the values given by Rudnick and Gao
 525 (2003) and by McLennan et al. (2006). Its uranium and thorium abundances are close to 40% of their respective
 526 primitive mantle values.

527

Table 1. Composition of the residual mantle

(1) Creation of an early-depleted reservoir (EDR) by extracting an early-enriched basaltic reservoir (EER). The EER is generated from primitive mantle by batch melting ($F = 10\%$) and sequestering a mantle mass fraction of $X(\text{EER}) = 0.022$ of this melt

(2) Differentiation of EDR into continental crust and Residual Mantle (RM)
This Table also shows published estimates of Depleted Mantle (DM) compositions for comparison

	Primitive Mantle	F(eer) = 0.1 X(eer) = 0.022	After EER extraction	Cont. Crust normalized			Residual Mantle, this paper	Depleted Mantle, Literature	Depleted Mantle, Literature	Depleted Mantle, Literature
				RG ²	MTH ²	Average (RG+MTH)	Average crust (RG & MTH)	SS ³	WH ³	BC ³
	C(eer)norm	C(edr)norm	C(cc)norm	C(cc)norm	C(cc)norm	C(rm)norm	C(dmm)norm	C(dmm)norm	C(dmm)norm	
Rb	0.6	9.98	0.798	81.67	81.67	81.67	0.328	0.147	0.083	0.167
Ba	6.6	10.00	0.797	69.09	37.88	53.48	0.448	0.182	0.085	0.208
Th	0.0795	9.89	0.800	70.44	52.83	61.64	0.396	0.172	0.099	0.201
U	0.0203	9.85	0.801	64.04	54.19	59.11	0.414	0.232	0.156	0.266
Nb ¹	0.555	9.74	0.803	14.41	14.41	14.41	0.713	0.319	0.226	0.432
Ta	0.037	9.74	0.803	18.92	21.62	20.27	0.674	0.373	0.259	
La	0.648	9.68	0.805	30.86	24.69	27.78	0.626	0.361	0.296	0.401
Ce	1.675	9.35	0.812	25.67	19.70	22.69	0.667	0.461	0.329	0.519
Pb	0.15	9.27	0.814	73.33	53.33	63.33	0.399	0.155	0.122	0.233
Pr	0.254	9.27	0.814	19.29	15.35	17.32	0.704	0.516	0.420	
Nd	1.25	9.07	0.818	16.00	12.80	14.40	0.728	0.570	0.465	0.645
Sm	0.406	7.84	0.846	9.61	8.62	9.11	0.791	0.665	0.588	0.722
Zr	10.5	8.46	0.832	12.57	9.52	11.05	0.764	0.756	0.484	
Hf	0.283	7.67	0.850	13.07	10.60	11.84	0.777	0.703	0.555	0.767
Eu	0.154	7.49	0.854	7.14	7.14	7.14	0.812	0.695	0.624	0.747
Gd	0.544	7.91	0.844	6.80	6.07	6.43	0.807	0.726	0.658	0.776
Tb	0.099	7.72	0.849	6.06	6.06	6.06	0.814	0.758	0.704	
Dy	0.674	7.57	0.852	5.34	5.49	5.42	0.822	0.788	0.749	
Ho	0.149	7.05	0.864	5.17	5.23	5.20	0.835	0.819	0.772	
Er	0.438	6.66	0.872	4.79	5.02	4.91	0.846	0.847	0.795	0.881
Yb	0.441	5.97	0.888	4.31	4.99	4.65	0.863	0.909	0.827	0.909
Lu	0.0675	5.40	0.901	4.44	4.44	4.44	0.877	0.933	0.859	0.933

1) The primitive mantle value of Nb = 0.658 given by McDonough and Sun (1995) has been adjusted to Nb = 0.555 ppm (see text).

2) Crustal compositions: RG = Rudnick and Gao (2003); MTH = McLennan et al., (2006)

3) Previously published Depleted Mantle values: SS = Salters and Stracke (2004); WH = Workman and Hart (2005); BC = Boyet and Carlson (2006)
Partition coefficients are for spinel lherzolite (Salters and Stracke, 2004)

528

529 5. Is the Early Enriched Reservoir hiding in the LLSVPs?

530 Finally, we briefly discuss the possibility that the Early Enriched Reservoir may be located near the core-
531 mantle boundary, within the LLSVPs (Large Low Shearwave Velocity Provinces), as shown in our cartoon of
532 mantle evolution (Figure 12). The LLSVPs have been recognized and delineated by seismologists relatively recently
533 (e.g. Dziewonski et al., 2010; Garnero & McNamara, 2008). Their estimated mass ranges from 2% (Burke et al.,
534 2008) to 9% of the silicate Earth (Cottaar & Lekic, 2016). Their ages have been traced by geological evidence from
535 hotspots and kimberlite for at least 300 Ma (Burke et al. 2008), but their actual age is essentially unknown; thus it
536 might well approach the age of the Earth. Most workers agree that the LLSVPs are compositionally different from
537 the surrounding and overlying mantle rocks. It is therefore possible that an early-enriched reservoir, as well as an
538 essentially primitive reservoir, have survived in these LLSVPs (e.g. Lau et al., 2017). For example, Ballmer et al.
539 (2016) propose a geodynamic model whereby the lower portion of the LLSVP is primitive, and the upper portion
540 consists of recycled basaltic crust. Although our simplified four-reservoir treatment does not specifically address
541 these issues, it is consistent with the existence of LLSVPs possessing a relatively complex internal structure and
542 compositional contrasts. Recent noble gas analyses of Xe, Ne and He in Iceland basalts compared with MORB also
543 demand the formation and survival of an EER to explain the observed isotopic distinctions (e.g. Mukhopadhyay,
544 2012). We suggest that the noble gases contained in the EER leak into the mantle-plume sources by diffusion. This
545 is consistent with dynamic Earth models in which plumes are derived predominantly from the boundary layer above

546 the LLSVPs, because the refractory elements in mantle plumes are dominated by recycled oceanic lithosphere that is
 547 significantly younger than the EER and possesses elevated (Nb,Ta)/U ratios caused by the extraction of continental
 548 crust.

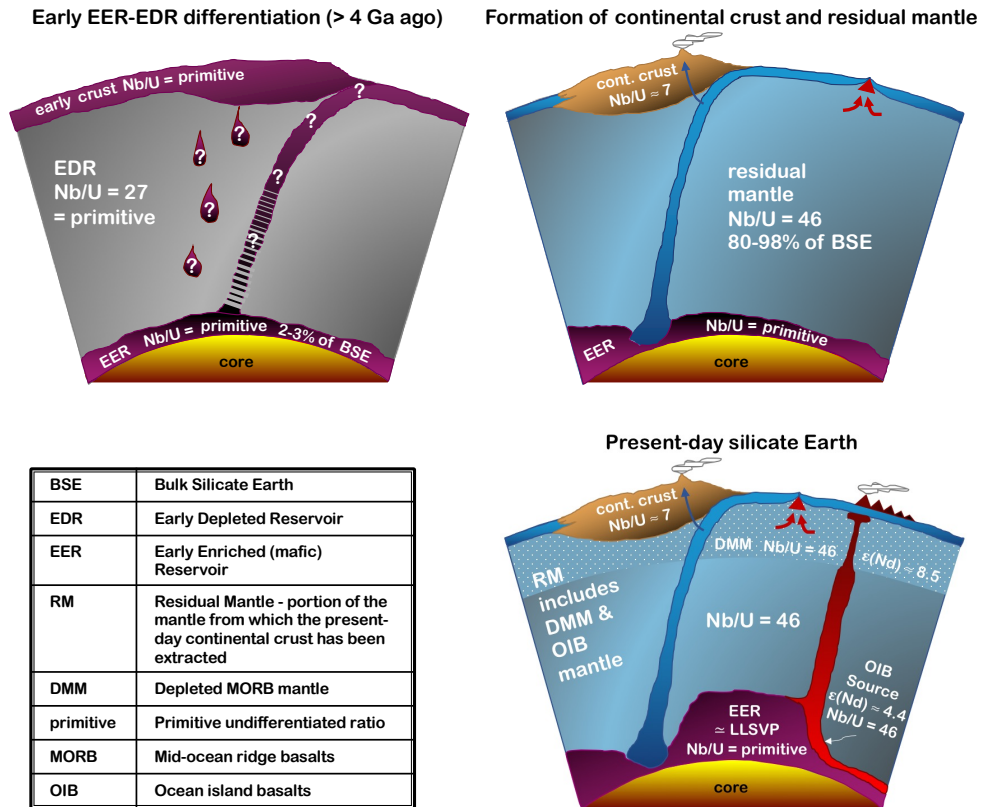


Fig. 11

549
 550 Fig.11. Cartoon of a possible crust-mantle evolution consistent with the constraints imposed by the
 551 combined evaluation of $\epsilon(\text{Nd})$ and (Nb,Ta)/U-based mass balances. (a) Initial differentiation of the
 552 primitive mantle into an EER (Early-Enriched Reservoir) by forming and subducting a mafic early
 553 (possibly primordial) crust, leaving behind a slightly depleted Early Depleted mantle (EDR) with primitive
 554 (Nb,Ta)/U but fractionated Sm/Nd. (b) Subsequent differentiation of the EDR into continental crust having
 555 Nb/U = 7 and a Residual Mantle Reservoir (RM) having Nb/U = 46. In this particular version, the RM
 556 occupies all of the mantle except the EER, but the uncertainties of the model allow up to about 30% EDR
 557 surviving in the mantle. Present day mantle: the residual mantle has undergone additional differentiation
 558 into MORB and OIB sources, and the EER has accumulated in the two LLSVPs in the lowermost mantle.

559

560 6. Summary

561 We have reevaluated the global crust-mantle differentiation of the classical three-reservoir (primitive
562 mantle, depleted MORB-mantle, continental crust) silicate Earth. We have found that no version of this model is
563 able to simultaneously account for the observed (Nb,Ta)/U and the $\epsilon(\text{Nd})$ -relationships used as measures of crust-
564 mantle differentiation.

565 The conflicting mass balance constraints can be reconciled with a four-reservoir Earth model (Fig. 11)
566 including an additional, early-enriched mantle reservoir (EER), now hidden within the Earth or lost to space, and its
567 complement, the early-depleted reservoir (EDR – Fig.11a). We assume that these reservoirs formed early in Earth
568 history, and Nb/U and Ta/U ratios in the EER and EDR are not fractionated relative to the primitive mantle (27.34
569 and 1.82, respectively). The EDR serves as the source for the continental crust (Fig. 11b). Nb/U and Ta/U ratios are
570 fractionated during continent formation. The residue of continental crust formation over geologic time from the
571 EDR is the Residual Mantle, which occupies at least 70% of the total mantle, and it may occupy all of it, except for
572 the EER itself. This means that less than 30%, and quite possibly none, of the original EDR survives to the present
573 day. To our knowledge, there are currently no hotspots that could be directly traced to an EDR source characterized
574 by their primitive Nb/U ≈ 30 , it seems plausible that all of the original EDR has been differentiated into continental
575 crust and present-day Residual Mantle.

576 The EER and possible remnants of the EDR may reside in the present-day LLSVP. They are likely to have
577 originated by the differentiation of an early mafic crust characterized by a lower-than-primitive Sm/Nd ratio but
578 primitive (Nb,Ta)/U ratios. The EER is conceptually similar to that postulated by Tolstikhin and Hofmann (2005) on
579 the basis of xenon isotopes and by Boyet and Carlson (2005) on the basis of ^{142}Nd isotopes, but its composition
580 differs significantly from the specific EERs postulated by Boyet and Carlson (2005) and Carlson and Boyet (2008)
581 and from the collisionally eroded crust of O'Neill and Palme (2008) and of Jackson and Jellinek (2013).
582 Alternatively, our results are consistent with models of deep burial of the EER or with its removal from the Earth by
583 collisional erosion.

584 In conclusion, classical $\epsilon(\text{Nd})$ -based estimates of the size and composition of the depleted mantle are
585 systematically in error. We have shown that no simple 3-reservoir mantle model consisting of a chondrite-derived,
586 primitive reservoir, a continental crust, and a depleted mantle reservoir is simultaneously consistent with the mass-
587 balance constraints imposed by the observed Nd isotopic compositions and the (Nb,Ta/U) ratios of mantle and crust.
588 This discrepancy exists whether the Nd isotopic mass balance takes into account only MORB or both MORB+OIB.

589 The Residual Mantle is much less depleted in highly incompatible elements, in particular the heat
590 producers Th and U, than given by the classical Nd isotope-based estimates. Thus, the heat production of the
591 present-day Residual Mantle, comprising both MORB and OIB sources, is about 40-50% of the bulk silicate value,
592 rather than 10–20% as estimated by traditional, isotope-based models. The distribution of these heat sources
593 between the relatively more enriched OIB sources and the more depleted MORB sources should be a subject of
594 future investigations.

595 **Acknowledgments**

596 We are grateful for the help given by Lucia Profeta of EarthChem to place our rather unwieldy
597 collection of global OIB data collected mostly from the GEOROC database into the EarthChem
598 data repository. Sunna Hardardottir kindly provided her database for geochemical data from
599 historic eruptions from Iceland. We also thank Rick Carlson, Francis Albarède, Charlie
600 Langmuir and an anonymous reviewer of an earlier submission of this work. These reviews
601 helped us prepare a largely rewritten manuscript and a more rigorous analysis of the range of
602 possible solutions to the global mass balance problem.

603 We will provide additional appropriate Acknowledgments upon acceptance of the manuscript.

604

605 **Open Research**

606 There are no original data presented in this paper. All geochemical data presented are from the
607 literature and are referenced.

608

609 **References**

- 610 Allègre, C.J., Brévar, O., Dupré, B. Minster, J.F., Isotopic and chemical effects produced in a
611 continuously differentiating convecting earth mantle. *Phil Trans. R. Soc. London Ser. A.*,
612 297, 447-477.
- 613 Anderson, M., Wanless, V.D., Perfit, M., Conrad, E. Gregg, P. Fornari, D. Ridley, W. I. (2021)
614 Extreme heterogeneity in mid-ocean ridge mantle revealed in lavas from the 8°20'N near-
615 axis seamount chain. *Geochemistry, Geophysics, Geosystems*, 22, e2020GC009322,
616 doi.org/10.1029/2020GC009322
- 617 Arevalo Jr, R., & McDonough, W. F. (2010). Chemical variations and regional diversity
618 observed in MORB. *Chemical Geology*, 271(1-2), 70-85.
- 619 Ballmer, M. D., Schumacher, L., Lekic, V., Thomas, C., & Ito, G. (2016). Compositional
620 layering within the large low shear-wave velocity provinces in the lower mantle.
621 *Geochemistry, Geophysics, Geosystems*, 17(12), 5056-5077.
- 622 Barth, M.G., McDonough, W.F., Rudnick, R.L. (2000) Tracking the budget of Nb and Ta in the
623 continental crust. *Chem. Geol.* 165, 197-213.
- 624 Boyet, M., & Carlson, R. W. (2005). 142Nd Evidence for Early (>4.53 Ga) Global
625 Differentiation of the Silicate Earth. *Science*, 309(5734), 576-581.
- 626 Boyet, M. & Carlson, R.W. (2006). A new geochemical model for the Earth's mantle inferred
627 from 146Sm-142Nd systematics. *Earth and Planetary Science Letters*, 254, 264-268.

- 628 Büchl, A., Münker, C., Mezger, K., & Hofmann, A. W. (2002). High-precision Nb/Ta and Zr/Hf
629 ratios in global MORB. *Geochimica et Cosmochimica Acta*, 66 Suppl.A, A 108.
- 630 Burke, K., Steinberger, B., Torsvik, T. H., & Smethurst, M. A. (2008). Plume Generation Zones
631 at the margins of Large Low Shear Velocity Provinces on the core-mantle boundary.
632 *Earth and Planetary Science Letters*, 265(1-2), 49-60.
- 633 Burkhardt, C., Borg, L. E., Brennecka, G. A., Shollenberger, Q. R., Dauphas, N., & Kleine, T.
634 (2016). A nucleosynthetic origin for the Earth's anomalous ¹⁴²Nd composition. *Nature*,
635 537(7620), 394-398. Letter
- 636 Campbell, I. H. (2002). Implications of Nb/U, Th/U and Sm/Nd in plume magmas for the
637 relationship between continental and oceanic crust formation and the development of the
638 depleted mantle. *Geochim. Cosmochim. Acta*, 66, 1651-1661.
- 639 Carlson, R. W., & Boyet, M. (2008). Composition of Earth's interior: The importance of early
640 events. *Phil. Trans. R. Soc. Lond. A*, 366, 4077-4103.
- 641 Caro, G. (2011). Early silicate earth differentiation. *Annu. Rev. Earth Planet. Sci.*, 39, 31-58.
- 642 Chauvel, C., Garçon, M., Bureau, S., Besnault, A., Jahn, B.-m., & Ding, Z. (2014). Constraints
643 from loess on the Hf-Nd isotopic composition of the upper continental crust. *Earth and
644 Planetary Science Letters*, 388(0), 48-58.
- 645 Christensen, U. R., & Hofmann, A. W. (1994). Segregation of subducted oceanic crust in the
646 convecting mantle. *J. Geophys. Res.*, 99, 19,867-819,884.
- 647 Cottaar, S., & Lekic, V. (2016). Morphology of seismically slow lower-mantle structures.
648 *Geophysical Journal International*, 207(2), 1122-1136.
- 649 Condie, K.C. & Shearer, C.K. (2017) Tracking the evolution of mantle sources with
650 incompatible element ratios in stagnant-lid and plate-tectonic planets. *Geochim.
651 Cosmochim. Acta*, 213, 47-62.
- 652 Davies, G. F. (1981). Earth's neodymium budget and structure and evolution of the mantle.
653 *Nature*, 290, 208-213.
- 654 DePaolo, D. J., & Wasserburg, G. J. (1976). Inferences about Magma Sources and Mantle
655 Structure from Variations of ¹⁴³Nd/¹⁴⁴Nd. *Geophys. Res. Lett.*, 3(12), 743-746.
- 656 DePaolo, D.J. (1980). Crustal growth and mantle evolution: inferences from models of element
657 transport and Nd and Sr isotopes. *Geochim. Cosmochim. Acta* 44, 1185-1196
- 658 Dziewonski, A. M., Lekic, V., & Romanowicz, B. A. (2010). Mantle Anchor Structure: An
659 argument for bottom up tectonics. *Earth and Planetary Science Letters*, 299(1-2), 69-79.
- 660 Farley KA, Natland JH, Craig H (1992) Binary mixing of enriched and undegassed (primitive?)
661 mantle components (He, Sr, Nd,Pb) in Samoan lavas. *Earth Planet Sci Lett* 111:183-199
- 662 Farnetani, C.G. and Richards, M. (1995) Thermal entrainment and melting in mantle plumes.
663 *Earth Planet. Sci. Lett.* 136, 251-267.
- 664 Fitton, J.G. & Godard, M. (2004) Origin and evolution of magmas from the Ontong Java Plateau.
665 *Geol. Soc. London Spec. Pub.* 229, 151-178.
- 666 Gale, A., Dalton, C. A., Langmuir, C. H., Su, Y., & Schilling, J.-G. (2013). The mean
667 composition of ocean ridge basalts. *Geochemistry, Geophysics, Geosystems*, 14, 489-518.
- 668 Garçon, M., Carlson, R. W., Shirey, S. B., Arndt, N. T., Horan, M. F., & Mock, T. D. (2017).
669 Erosion of Archean continents: The Sm-Nd and Lu-Hf isotopic record of Barberton
670 sedimentary rocks. *Geochimica et Cosmochimica Acta*, 206(Supplement C), 216-235.
- 671 Garnero, E. J., & McNamara, A. K. (2008). Structure and Dynamics of Earth's Lower Mantle.
672 *Science*, 320(5876), 626-628.

- 673 Gast, P. W. (1968). Trace element fractionation and the origin of tholeiitic and alkaline magma
674 types. *Geochim. Cosmochim. Acta*, 32, 1057-1086.
- 675 Goldstein, & Jacobsen, S. B. (1988). Nd and Sr isotopic systematics of river water suspended
676 material: implications for crustal evolution. *Earth and Planetary Science Letters*, 87(3),
677 249-265.
- 678 Goldstein, S. L., O'Nions, R. K., & Hamilton, P. J. (1984). A Sm-Nd isotopic study of
679 atmospheric dusts and particulates from major river systems. *Earth Planet. Sci. Lett.*, 70,
680 221-236.
- 681 Hacker, B. R., Kelemen, P. B., & Behn, M. D. (2015). Continental lower crust. *Annu. Rev. Earth
682 Planet. Sci.*, 43, 167-205.
- 683 Hauri, E.H., Whitehead, J.A., Hart, S.R. (1994) Fluid dynamic and geochemical aspects of the
684 entrainment in mantle plumes. *J. Geophys. Res.* 99, 24275-24300.
- 685 Hart, S. R. (1971). K, Rb, Cs, Sr, Ba contents and Sr isotope ratios of ocean floor basalts. *Philos.
686 Trans. R. Soc. London. Ser. A.*, 268, 573-587.
- 687 Hoernle, K., Hauff, F. van den Bogaard, P., Werner, R., Mortimer, N. Geldmacher, J., Garbe-
688 Schönberg, D. Davy, B. (2010). Age and geochemistry of volcanic rocks from the
689 Hikurangi and Manihiki oceanic plateaus. *Geochim. Cosmochim. Acta*, 74, 7196-7219.
- 690 Hart, S.R., Hauri, E.H. Oschmann, L.A., Whitehead, J.A. (1982). Mantle plumes and
691 entrainment. *Science* 256, 517-520.
- 692 Hofmann, A. W. (1988). Chemical differentiation of the Earth: the relationship between mantle,
693 continental crust, and oceanic crust. *Earth Planet. Sci. Lett.*, 90, 297-314.
- 694 Hofmann, A. W. (1989). Geochemistry and models of mantle circulation. *Phil. Trans. R. Soc.
695 Lond. A*, 328, 425-439.
- 696 Hofmann, A. W. (2003). Sampling mantle heterogeneity through oceanic basalts: Isotopes and
697 trace elements. In R. W. Carlson (Ed.), *Vol. 2 The Mantle and Core* (Vol. 2, pp. 61-101).
698 Oxford: Elsevier-Pergamon.
- 699 Hofmann, A. W. (2014). 3.3 - Sampling Mantle Heterogeneity through Oceanic Basalts: Isotopes
700 and Trace Elements. In H. D. Holland & K. K. Turekian (Eds.), *Treatise on
701 Geochemistry (Second Edition)* (pp. 67-101). Oxford: Elsevier.
- 702 Hofmann, A. W., Jochum, K.-P., Seufert, M., & White, W. M. (1986). Nb and Pb in oceanic
703 basalts: new constraints on mantle evolution. *Earth Planet. Sci. Lett.*, 79, 33-45.
- 704 Hofmann, A. W., & White, W. M. (1980). The role of subducted oceanic crust in mantle
705 evolution. *Carnegie Inst. Wash. Year Book*, 79, 477-483.
- 706 Hofmann, A. W., & White, W. M. (1982). Mantle plumes from ancient oceanic crust. *Earth
707 Planet. Sci. Lett.*, 57, 421-436.
- 708 Hofmann, A. W., & White, W. M. (1983). Ba, Rb, and Cs in the Earth's mantle. *Z. Naturforsch.*,
709 38, 256-266.
- 710 Homrighausen, S., Hoernle, K., Hauff, F., Geldmacher, J., Wartho, J.-A., van den Bogaard, P.,
711 Garbe-Schönberg, D. (2018) Global distribution of the HIMU end member: Formation
712 through Archean plume-lid tectonics. *Earth Science Reviews* 182, 85-101.
- 713 Huang, D. Badro, J., Siebert, J. (2020) The niobium and tantalum concentration in the mantle
714 constrains the composition of Earth's primordial magma ocean. *Proc. Natl. Acad. Sci.*
715 117, 27893-27898.
- 716 Jackson, M. G., Hart, S. R., Koppers, A. A. P., Staudigel, H., Konter, J., Blusztajn, J., et al.
717 (2007). The return of subducted continental crust in Samoan lavas. *Nature*, 448(7154),
718 684-687.

- 719 Jackson, M.G. Jellinek, A.M. (2013) Major and trace element composition of the high $^3\text{He}/^4\text{He}$
720 mantle: Implications for the composition of a nonchondritic Earth. *G-Cubed* 14, 2954-
721 2976
- 722 Jacobsen, S. B., & Wasserburg, G. J. (1979). The mean age of mantle and crustal reservoirs. *J.*
723 *Geophys. Res.*, 84, 7411-7427.
- 724 Jenner, F. E., & O'Neill, H. S. C. (2012a). Analysis of 60 elements in 616 ocean floor basaltic
725 glasses. *Geochem. Geophys. Geosyst.*, 13, Q02005.
- 726 Jenner, F. E., & O'Neill, H. S. C. (2012b). Major and trace analysis of basaltic glasses by laser-
727 ablation ICP-MS. *Geochem. Geophys. Geosyst.*, 13, Q03003.
- 728 Klein, E. M., & Langmuir, C. H. (1987). Global correlations of ocean ridge basalt chemistry with
729 axial depth and crustal thickness. *J. Geophys. Res.*, 92, 8089-8115.
- 730 Kurz, M. D., Jenkins, W. J., & Hart, S. R. (1982). Helium isotopic systematics of oceanic
731 islands: implications for mantle heterogeneity. *Nature*, 297, 43-47.
- 732 Lau, H. C. P., Mitrovica, J. X., Davis, J. L., Tromp, J., Yang, H.-Y., & Al-Attar, D. (2017). Tidal
733 tomography constrains Earth's deep-mantle buoyancy. *Nature*, 551, 321. Article
- 734 Madrigal, P. Gazel, E. Flores, K. E., Bizimis, M., Jicha, B. (2016) Record of massive upwellings
735 from the Pacific large low shear velocity province. *Nature Communications* 7, 13309.
- 736 McDonough, W. F., & Sun, S.-S. (1995). The composition of the Earth. *Chem. Geol.*, 120, 223-
737 253.
- 738 McLennan, S. M., Taylor, S. R., & Hemming, S. R. (2006). Composition, differentiation, and
739 evolution of continental crust: Constraints from sedimentary rocks and heat flow. In M.
740 Brown & T. Rushmer (Eds.), *Evolution and Differentiation of the Continental Crust* (pp.
741 92-134): Cambridge Univ. Press.
- 742 Mukhopadhyay, S. (2012). Early differentiation and volatile accretion recorded in deep-mantle
743 neon and xenon. *Nature*, 486(7401), 101-104. 10.1038/nature11141
- 744 Münker, C., Fonseca, R. O. C., & Schulz, T. (2017). Silicate Earth's missing niobium may have
745 been sequestered into asteroidal cores. *Nature Geoscience*, 10, 822. Article
- 746 Münker, C., Pfänder, J. A., Weyer, S., Büchl, A., Kleine, T., & Mezger, K. (2003). Evolution of
747 planetary cores and the earth-moon system from Nb/Ta systematics. *Science*, 301(5629),
748 84-87.
- 749 O'Neill, H. S. C., & Palme, H. (2008). Collisional erosion and the non-chondritic composition of
750 the terrestrial planets. *Phil. Trans. R. Soc. A*, 366, 4205-4238.
- 751 O'Nions, R. K., Evensen, N. M., & Hamilton, P. J. (1977). Variations in $^{143}\text{Nd}/^{144}\text{Nd}$ and
752 $^{87}\text{Sr}/^{86}\text{Sr}$ ratios in oceanic basalts. *Earth Planet. Sci. Lett.*, 34, 13-22.
- 753 O'Nions, R. K., Evensen, N. M., & Hamilton, P. J. (1979). Geochemical modeling of mantle
754 differentiation and crustal growth. *J. Geophys. Res.*, 84, 6091-6101.
- 755 Pfänder, J. A., Münker, C., Stracke, A., & Mezger, K. (2007). Nb/Ta and Zr/Hf in ocean island
756 basalts -- Implications for crust-mantle differentiation and the fate of Niobium. *Earth and*
757 *Planetary Science Letters*, 254(1-2), 158-172.
- 758 Plank, T. (2014). The Chemical Composition of Subducting Sediments. In H. D. Holland & K.
759 K. Turekian (Eds.), *Treatise on Geochemistry (Second Edition)* (Vol. 4.17, pp. 607-629).
760 Oxford: Elsevier.
- 761 Rudnick, R. L. (1990). Nd and Sr isotopic compositions of lower-crustal xenoliths from north
762 Queensland, Australia: Implications for Nd model ages and crustal growth processes.
763 *Chem. Geol.*, 83(3/4), 195-208.

- 764 Rudnick, R. L., & Fountain, D. M. (1995). Nature and composition of the continental crust: a
765 lower crustal perspective. *Rev. Geophysics*, 33, 267-309.
- 766 Rudnick, R. L., & Gao, S. (2003). Composition of the continental crust. In R. L. Rudnick (Ed.),
767 *Treatise on Geochemistry* (Vol. 3 The Crust, pp. 1-64): Elsevier.
- 768 Rudnick, R. L., & Goldstein, S. L. (1990). The Pb isotopic compositions of lower crustal
769 xenoliths and the evolution of lower crustal Pb. *Earth Planet. Sci. Lett.*, 98, 192-207.
- 770 Salters, V. J. M., & Stracke, A. (2004). Composition of the depleted mantle. *Geochem. Geophys.*
771 *Geosystems*, 5, doi:10.1029/2003GC000597.
- 772 Sims, K. W. W., & DePaolo, D. J. (1997). Inferences about mantle magma sources from
773 incompatible element concentration ratios in oceanic basalts. *Geochim. Cosmochim.*
774 *Acta*, 61, 765-784.
- 775 Sleep, N. H. (1990). Hotspots and mantle plumes: Some phenomenology. *J. Geophys. Res.*, 95,
776 6715-6736.
- 777 Sun, S. S., & Hanson, G. N. (1975). Evolution of the mantle: Geochemical evidence from alkali
778 basalt. *Geology*, 3, 297-302.
- 779 Taylor, S. R., & McLennan, S. M. (1985). *The continental crust: its composition and evolution.*
780 Oxford: Blackwell Scientific Publications.
- 781 Trela, J., Gazel, E., Sobolev, A. V., Moore, M., Bizimis, M., Jicha, B. Batanova, B.G. (2017) The
782 hottest lavas of the Phanerozoic and the survival of deep Achaean reservoirs. *Nature*
783 *Geoscience* 10, 451-456.
- 784 Tolstikhin, I. N., & Hofmann, A. W. (2005). Early Crust on top of the Earth's core. *Phys. Earth*
785 *Planet. Interiors*, 148, 109-130.
- 786 Turner, S. J., & Langmuir, C. H. (2015). The global chemical systematics of arc front
787 stratovolcanoes: Evaluating the role of crustal processes. *Earth and Planetary Science*
788 *Letters*, 422(0), 182-193.
- 789 Wade, J., & Wood, B. J. (2001). The Earth's 'missing' niobium may be in the core. *Nature*, 409,
790 75-78.
- 791 Wänke, H., Baddenhausen, H., Dreybus, G., Jagoutz, E., Kruse, H., & Palme, H. (1973).
792 Multielement analyses of Apollo 15, 16, and 17 samples and the bulk composition of the
793 moon. *Proceedings of the Fourth Lunar Science Conference (Suppl 4, Geochim.*
794 *Cosmochim. Acta)*, 2, 1461-1481.
- 795 Wasserburg, G. J., & DePaolo, D. J. (1979). Models of Earth Structure Inferred from
796 Neodymium and Strontium Isotopic Abundances. *Proc. Natl. Acad. Sci. U. S. A.*, 76(8),
797 3594-3598.
- 798 Workman, R. K., & Hart, S. R. (2005). Major and trace element composition of the depleted
799 MORB mantle (DMM). *Earth and Planetary Science Letters*, 231(1-2), 53-72.
- 800 Zindler, A., Jagoutz, E., & Goldstein, S. L. (1982). Nd, Sr, and Pb isotopic systematics of a
801 three-component mantle: a new perspective. *Nature*, 298, 519-523.
- 802